A Criterion for Optimal Design of Multi-Axis Force Sensors

Antonio Bicchi

Dipartimento di Sistemi Elettrici e Automazione (DSEA)
and Centro "E. Piaggio"
Facoltà di Ingegneria, Universitá di Pisa

Abstract

This paper deals with the design of multi-axis force (also known as force/torque) sensors, as considered within the framework of optimal design theory. Optimal design procedures consist of finding the combination of design variables that extremizes some optimality criterion: provided a suitable mathematical formulation of the problem, solutions can be efficiently obtained through currently available numerical techniques. The principal goal of this paper is to identify a mathematical objective function, whose minimization corresponds to the optimization of sensor accuracy. The methodology employed is derived from linear algebra and analysis of numerical stability. An objective function which can be applied to a large class of sensor configurations is proposed. The problem of optimizing the number of basic transducers employed in a multi-component sensor is also addressed. Finally, applications of the proposed method to the design of a simple sensor as well as to the optimization of a novel, 6-axis miniaturized sensor are discussed.

1 Introduction

The development of multi-axis force sensors, i.e. instruments for measuring several (up to 6) components of force and torque simultaneously, has been initially undertaken in fields such as wind-tunnel testing, adaptive control of machines and thrust stand testing of rocket engines. Typical in those areas is the problem of monitoring forces of variable directions and intensity. Some of the most interesting sensors designed in this phase are reviewed by Doebelin [1]. Starting from the mid seventies, a major impulse to research on such sensors has been given by the recognition of their large relevance to robotic and telemanipulation applications.

The ability to sense the arm-environment interactions is a crucial need for robots to evolve from purely repetitive behaviors to some degree of autonomy in unstructured surroundings or tasks. The feed-back of forces and torques exerted by the arm's end effector is not only instrumental for the accomplishment of most tasks involving modification of the environment by contact, but is also critical in guaranteeing safe operation of the arm.

Considering the most common case of a serial link manipulator, a complete characterization of the system of forces acting on a portion of the arm can be obtained by force sensors interposed between that portion and the rest of the arm. Force sensing at intermediate sections of the kinematic chain is likely to be very useful for next-generation robots using the whole arm surface to interact with the environment [2, 3]. However, since the measurement of interaction forces can be disturbed by inertial forces arising from acceleration of the masses between the sensor and the end-effector, force sensors are usually placed as close as possible to the distal end of

1

the arm, most often at the wrist. Several configurations have been proposed for such sensorized wrists (e.g. [4, 5, 6]), and some are commercially available. A pedestal force sensor has also been described in [4].

The increasingly demanding tasks assigned to automatic manipulation require ever more stringent accuracy, stiffness, encumbrance, weight, speed of response, ease of interfacing and reliability of force sensors for robotics. A particularly promising application of force sensing to fine manipulation, for instance, is the so-called intrinsic contact sensing concept [7, 8]. Very detailed information about the contact between two surfaces can be obtained based on force measurements and geometric considerations. By integrating force sensors in the very "fingertips" of the arm, interactions with manipulated objects can be monitored very closely. The improvement in manipulation dexterity has proven considerable for both simple parallel jaw grippers [9], and for dextrous articulated hands [10, 11, 12]. A drastic reduction of size and weight of the force sensors with respect to existing designs turned out to be mandatory for this application.

The stringent and conflicting requirements of this and other advanced applications of force sensing render unsatisfactory the traditional, intuitive approach to force sensor design, and motivated the investigation of a more systematic approach. In this paper the design of multi-axis force sensors is considered within the framework of optimal design theory, the branch of operations research currently offering the most developed tool for systematic synthesis of optimized designs.

2   Problem Formulation

According to Vanderplaats [13], an optimal design problem (which is basically a nonlinear programming problem) can be stated as follows:

Find the set of r design variables x_i that minimizes the objective function $F(\mathbf{x})$, subject to:

1. p inequality constraints: $g_i(\mathbf{x}) \leq 0$, $1 \leq i \leq p$;
2. q absolute constraints: $h_j(\mathbf{x}) = 0$, $1 \leq j \leq q$;
3. n bounds defining the feasible design region: $x_{k,inf} \leq x_k \leq x_{k,sup}$, $1 \leq k \leq n$.

The variables characterizing a force sensor design can be chosen within a large range of quantities related to its geometric description, dimensions, material properties, machining process, transduction principle, etc.. Any quantity contributing to the identification of a design, which is not allowed to vary in the optimization process, is considered a design parameter.

Inequality conditions are unilateral constraints that must be satisfied in order for the design to be acceptable. For example, stresses in structure members must not exceed specified values. The maximum displacement under nominal load, and the the minimum detectable load of the sensor can be conveniently considered under the form of inequality constraints.

By means of an equality constraint, precise conditions that must be met by the design can be stated. For instance, these constraints can be used to define the system interfaces. A complex problem can be reduced to a simpler sub-optimal one by using equality constraints to assign some variables a fixed value.

Finally, boundary constraints defining the feasible region for design variables prevent the optimization algorithm from converging to unacceptable solutions (e.g., sensor structure members with negative thickness).

The objective function $F(\mathbf{x})$ is the measure adopted for quantifying the quality of a design. A most important decision is implied by the choice of the quality to be optimized. In some

cases emphasis can be put on cost, encumbrance, or weight reduction. Very often, however, the accuracy of measurements is of paramount importance in designing a force sensor. It is possible to take into account these and other possible criteria at the same time by using multi-criteria optimization techniques [14], e.g. by assigning weighting factors to each criterion. Although greater flexibility of the optimization tool can be achieved in this way, there is a risk with multi-criteria techniques of loosing insight into the design process. In this paper, all the above mentioned and other possible requirements are considered as design constraints, and the focus is on the choice of an objective function capable of extracting, from the class of acceptable designs, the one giving best results in terms of measurement accuracy.

3   Mathematical Model of a Force Sensor

In general, a multi-axis force sensor is a device in which several simple transducers measure the effects of unknown loads on a mechanical structure. These basic measurements are processed in order to evaluate the components of the applied load. As far as a linear behavior can be hypothesized for the sensor, a model can be written as

$$\mathbf{v} = \mathbf{C}\mathbf{p} \tag{1}$$

where $\mathbf{p} \in \Re^n$, $n \leq 6$, is the unknown load vector, $\mathbf{v} \in \Re^m$, $m \geq n$ is a vector collecting the basic measurements, and $\mathbf{C} \in \Re^{m \times n}$ is a constant, full rank matrix characteristic of the sensor. The unknown vector $\mathbf{p}$ is composed of some or all the components of the resultant of the load; each component is normalized with respect to its maximum value, which is given as a design specification. When basic measurements are relative to strains or displacements (as it most often occurs in practical applications), the $\mathbf{C}$ matrix is usually referred to as the *compliance* matrix of the sensor.

The behavior assumed in equation 1 is ideal under several regards. For instance, the linearity assumption is rather strong. However, one is forced to such approximation by the need for a viable algorithm for *inverting* the model, i.e. for solving equation 1. Nonlinear elastic models of even simple mechanical structures are too complex for being inverted, and even though a tabulated calibration of a sensor is conceivable, there is no practical application of such technique to force sensors. As a matter of fact, linear (or piece-wise linear) approximations can be sharpened by calibration techniques (see e.g. [15]).

As a second remark about the model 1, we note that the actual measurement vector $\mathbf{v}$ will be in all likelihood affected by an error $\delta\mathbf{v}$ due to inaccuracies of basic transducers. Similarly, also the imprecise knowledge of the actual $\mathbf{C}$ matrix, which will be affected by a (matrix) error $\delta\mathbf{C}$, should be taken into account. Thus, a model for a real sensor should be written as

$$\mathbf{v} = (\mathbf{C} + \delta\mathbf{C})\mathbf{p} \; + \; \delta\mathbf{v} \tag{2}$$

To explain the origin of errors $\delta\mathbf{v}$ and $\delta\mathbf{C}$, consider for instance a sensor using strain gauges. As is well known, strain gauges are electrical resistors that can be bonded on a deformable structure, and vary their resistance according to the mechanical strain of the structure. Errors $\delta\mathbf{v}$ in evaluation of structure strains can be caused by electrical noise and thermal drift in resistance measurements, and by discretization errors in conversion of data from analog to digital. The elements of the compliance matrix $\mathbf{C}$ are in turn determined only approximately, either using elasticity theory formulas or a direct calibration procedure. Both these methods result in a relative error ϵ_c (usually much larger in the first case), arising from inappropriate modeling of sensor structure (for calculated $\mathbf{C}$'s), or from inaccuracies in calibration. The effects

of nonlinearities in the stress-strain relationship of the structure, the imperfect stiffness of the glue used to bond the gauges, and many other uncontrollable factors will also add to ϵ_c.

Multi-axis force sensors can be subdivided between those using the minimal number of basic transducers for the measure of the unknown load components (i.e., $m = n$), and those having redundant sensors ($m > n$). In the latter case, no exact solution of equation 1 is possible, and diverse approximate solutions can be chosen. This classification will be used in the following discussion.

4   Minimal Sensors

For $m = n$, the generalized form of Wilkinson's formula for error propagation in linear algebraic systems (see [16]) can be utilized in order to give an *a priori* estimate of the relative error on $\mathbf{p}$:

$$\epsilon_p = (\epsilon_v + \epsilon_c) \, K_p(\mathbf{C}), \tag{3}$$

where $\epsilon_v = \frac{\|\delta\mathbf{v}\|}{\|\mathbf{v}\|}$, $\epsilon_c = \frac{\|\delta\mathbf{C}\|}{\|\mathbf{C}\|}$, $\epsilon_p = \frac{\|\delta\mathbf{p}\|}{\|\mathbf{p}\|}$ are respectively the relative errors on strain measurements, on calibration and on the results (being $\delta\mathbf{p}$ the error resulting on the processed information from the sensor). The symbol $\|\cdot\|$ represents a generic vector norm, or the subordinate matrix norm if the argument is a matrix [1]. The propagation factor K_p has the upper bound:

$$K_p(\mathbf{C}) \leq \frac{N_C}{1 - N_C \epsilon_c}, \tag{4}$$

where N_C is the condition number of the compliance matrix $\mathbf{C}$, defined as

$$N_C = \|\mathbf{C}\| \, \|\mathbf{C}^{-1}\|,$$

and where it is assumed $N_C \, \epsilon_c < 1$. It appears from equation 4 that large condition numbers of $\mathbf{C}$ can spoil even the most accurately measured and calibrated sensor.

After its definition, $N_C \geq 1$, which implies $K_p > 1$: this can be seen as an instance of the general principle of information theory regarding the entropy increase due to elaboration of data [17]. In the best case, when $N_C = 1$ (which occurs only for orthogonal matrices and their multiplies), and $K_p = (1 - \epsilon_c)^{-1} \approx 1$, the global error ϵ_p is simply the sum of source errors ϵ_v and ϵ_c.

Given a sensor design, substantial reductions of ϵ_v and ϵ_c can be achieved only by using more sophisticated technologies, materials and components in the construction of the sensor, and finer models of the structure, or more accurate instrumentation for strain measurement and calibration. An improvement of these factors with respect to present sensors is therefore achievable by increasing their cost. Also assuming no cost constraint to the design, however, there are absolute upper bounds to possible reduction of source errors set by present technological state-of-art, and by inherent measurement accuracy limitations.

The amplification factor K_p in equation 3 is related to the elements of the compliance matrix $\mathbf{C}$, which can be chosen by the designer by varying, for instance, the thickness of some members in the structure, the position of strain-gauges, etc. Thus, the problem of optimizing the accuracy of multi-axis force sensors can be split in a technology-dominated sub-problem, and a design-dominated one.

It should be pointed out that equation 3 does not assume any specific algorithm for the solution of the linear system 1. From this viewpoint, different algorithms such as LU factorization,

---

[1]Vectors are designed by lower case boldface letters in this paper, while matrices are upper case boldface

singular value decomposition (SVD), and even special solution schemes relying on a possibly structured $\mathbf{C}$ matrix, are equivalent. The application of these methods with finite precision machines will produce numerical errors that are typically some orders of magnitude smaller than source errors, and can be considered as a small portion of the overall calibration error ϵ_c [18].

Since the right-hand member of equation 4 is a monotonic non-decreasing function of N_C, it seems natural to choose the condition number of the compliance matrix $\mathbf{C}$ as the objective function of the optimization procedure. This choice is indeed correct when only minimal sensors are taken into consideration. M. Uchiyama and K. Hakomori proposed the use of the condition number of the compliance matrix of a force sensor in [19]. Unfortunately, their work was published in Japanese, and it has not been as widely known as it deserved until cited by [20] [2]. The authors of [20] criticize the condition number criterion of [19] under four regards. Some of those points are discussed here, since this is believed to provide insight in the general problem of optimal design of force sensors.

The first remark is that the condition number criterion is insensitive to absolute values of the compliance matrix entries. In other words, $N(\mathbf{C}) = N(2\mathbf{C})$. While it is an obvious advantage of condition numbers to be scale-independent, the authors of [20] underscore the fact that sensors with larger absolute values of structural strains are not rewarded by this criterion. A design principle consisting in making the "strain-gauge sensitivity" as large as possible is proposed, which consists in maximizing the norm of the rows of $\mathbf{C}$. In other words, a sensor is optimal under this principle if, for the maximum nominal load, every gauge is strained at the maximum allowable level.

The second, third and fourth remarks to the condition number criterion all apply to the fact that it does not generalize to redundant sensors. For instance, the two compliance matrices $\mathbf{C}_1 = \begin{pmatrix} 1 & 0 \\ 0 & 1 \end{pmatrix}$ and $\mathbf{C}_2 = \begin{pmatrix} 1 & 0 \\ 1 & 0 \\ 0 & 1 \end{pmatrix}$ are brought to our consideration. The condition numbers are $N_{C_1} = 1$ and $N_{C_2} = \sqrt{2}$, respectively. The authors note that, "although $\mathbf{C}_2$ may have a redundant strain-gauge, $\mathbf{C}_2$ seems not to have less sensing performance than $\mathbf{C}_1$". This fact is true indeed, and it will be shown in the following sections that this problem (as well as the others pointed out by [20]) can be solved by a correct generalization of the condition number criterion to redundant sensors.

Two more design principles are proposed by the authors of [20], the first being to maximize the minimum singular value of the compliance matrix $\mathbf{C}$, and the second to minimize the maximum singular value of a displacement matrix $\mathbf{G}$, evaluated at the point of application of the load.

In the method presented in this paper we avoid the definition of multiple optimality criteria, in order to avoid the need of a difficult choice of weights, which always imply a degree of arbitrariness. A lower bound on sensitivity, as well as an upper bound on displacement under load, can be very easily incorporated as unilateral constraints to the design (see section 2 above and 7 below). On the other hand, an attempt is made at generalizing the condition number criterion for redundant sensors, as the single criterion able to synthesize accuracy requirements for the sensor (it can be seen for instance that maximizing strain gauge and force sensitivities as defined by [20] leads to minimizing the condition number).

---

[2] An independently developed formulation of the method has been presented at the same time in [11]

5 Redundant Sensors

Consider again equation 1, $\mathbf{v} = \mathbf{Cp}$, in the case that the number of independent measurements, m, is larger than the number of unknown load components, n. Since the entries of both $\mathbf{C}$ and $\mathbf{v}$ derive from experimental measurements, equation 1 is in any practical case inconsistent, i.e. no exact solution is possible. Only approximate solutions, denoted with $\tilde{\mathbf{p}}$, can be obtained through a manipulation of equation 1 as:

$$\mathbf{Mv} = \mathbf{MCp}, \tag{5}$$
$$\tilde{\mathbf{p}} = (\mathbf{MC})^{-1}\mathbf{Mv}, \tag{6}$$

where $\mathbf{M} \in \Re^{n \times m}$, and it is assumed that $\det(\mathbf{MC}) \neq 0$.

Such a manipulation consists of projecting the measured point $\mathbf{v}$ of the m-dimensional space onto the range space of $\mathbf{C}$, denoted with $\mathcal{R}(\mathbf{C})$, which is a n-dimensional subspace. The direction along which the projection is made is specified by the choice of $\mathbf{M}$. In particular, if $\mathbf{M} = \mathbf{C}^T$, the corresponding solution $\tilde{\mathbf{p}} = \mathbf{C}^\dagger \mathbf{v}$ (where $\mathbf{C}^\dagger = (\mathbf{C}^T\mathbf{C})^{-1}\mathbf{C}^T$ is the pseudo-inverse of $\mathbf{C}$) is the least squares solution to equation 1. Note that we used here the assumption that $\mathbf{C}$ is full rank, which is not restrictive at all insofar as reasonable sensor designs are considered.

Naturally, any minimal sensor can be considered as a particular case of a redundant one, by supposing that $(m-n)$ measurements are neglected. Correspondingly, and modulo a reordering of rows, a manipulation matrix $\mathbf{M} = (\mathbf{I}_{n \times n} | \mathbf{0}_{n \times (m-n)})$ is adopted in equation 5. Also for minimal sensors, therefore, the solution $\mathbf{p}$ is to be considered only an approximation of the "true" value of applied load.

The total error $\delta\mathbf{p}$ can hence be thought as a sum of two terms, deriving from the projective manipulation 5, and from the actual solution of 6, respectively. The rest of this paper will discuss the application of the generalized condition number criterion to the solution of equation 6: minimizing the error in its solution is assumed as the goal of design optimization. Before beginning such discussion, however, it seems appropriate to show that the error term deriving from the projection 5 is not directly affected by the choice of the compliance matrix $\mathbf{C}$ elements, but rather it depends only on the source errors, $\delta\mathbf{v}$ and $\delta\mathbf{C}$. In other words, the projection error is technology-dominated, while the solution error is design-dominated.

This fact can be graphically illustrated with reference to a very simple example with $m = 2$, $n = 1$. An hypothetical error-free sensor, modeled by the linear equation $\mathbf{v} = \mathbf{Cp}$, would have the measurement vector $\mathbf{v}$ lying exactly on $\mathcal{R}(\mathbf{C})$, represented in figure 1 with a dashed line. The "true" solution would be represented in this case by the length of the segment OZ. However, any solution of the real sensor sketched in equation 2 corresponds to a projection of the vector $\mathbf{v} = (\mathbf{C} + \delta\mathbf{C})\mathbf{p} + \delta\mathbf{v}$ onto $\mathcal{R}(\mathbf{C} + \delta\mathbf{C})$ (solid line in figure 1). Different manipulation matrices produce different approximate solutions. For instance, the length OA corresponds to the choice $\mathbf{M} = (1\ 0)$, i.e. to neglecting the second measurement; OC corresponds to $\mathbf{M} = (0\ 1)$, neglecting the first one; OB represents the least-squares approximation obtained with $\mathbf{M} = \mathbf{C}^T$. The "true" solution, of course unknowable, can now be represented by the length $OY = OZ$. The total error $\delta\mathbf{p}$ is the sum of a projection error (e.g., $OB - OY$ in the case of least squares), and of an algorithmic error, which propagates in solving equation 5 (i.e. in finding the length OB).

The sensor design, i.e. the choice of the elements of $\mathbf{C}$, place the subspace $\mathcal{R}(\mathbf{C})$ in $\Re^2$. By varying this choice, and keeping $\delta\mathbf{v}$ and $\delta\mathbf{C}$ constant, the projection error does not change, since this variation amounts to a rigid rotation of the graph of figure 1 about the point O. Therefore,
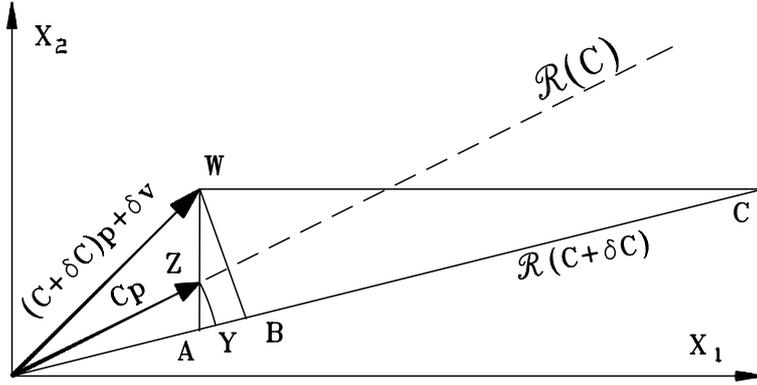
Figure 1: The projection error is not affected by the design of the compliance matrix.

it seems reasonable to apply design criteria that tend to optimize the accuracy in evaluating $\tilde{\mathbf{p}}$, the best affordable approximation of the "true" load with a given technological implementation.

Applying equation 3 to equation 5, we have

$$\epsilon_p = (\epsilon_{mv} + \epsilon_{mc})K_p(\mathbf{MC}), \tag{7}$$

where $\epsilon_{mv} = \frac{\|\delta(\mathbf{Mv})\|}{\|\mathbf{Mv}\|}$, $\epsilon_{mc} = \frac{\|\delta(\mathbf{MC})\|}{\|\mathbf{MC}\|}$.

In order to correctly compare sensors that employ different solution methods for equation 5, or even sensors built with different numbers of basic transducers but comparable technology, we need to express equation 7 explicitly in terms of relative source errors ϵ_v, ϵ_c. By "comparable technology" it is meant here that all basic transducers have the same statistical properties in terms of measurement and calibration accuracy, such that ϵ_v and ϵ_c are not varied by adding or removing transducers [3].

The term ϵ_{mc} can be rearranged as

$$\begin{aligned}
\epsilon_{mc} &= \frac{\|(\mathbf{M} + \delta\mathbf{M})(\mathbf{C} + \delta\mathbf{C}) - \mathbf{MC}\|}{\|\mathbf{MC}\|} \approx \\
&\approx \frac{\|\mathbf{M}\ \delta\mathbf{C} + \delta\mathbf{M}\ \mathbf{C}\|}{\|\mathbf{MC}\|} \leq \frac{\|\mathbf{M}\|\ \|\mathbf{C}\|}{\|\mathbf{MC}\|}\ (\epsilon_m + \epsilon_c),
\end{aligned}$$

where $\epsilon_m = \frac{\|\delta\mathbf{M}\|}{\|\mathbf{M}\|}$ is the relative error the matrix $\mathbf{M}$ is known with. As for the term ϵ_{mv}, it holds:

$$\begin{aligned}
\epsilon_{mv} &= \frac{\|(\mathbf{M} + \delta\mathbf{M})(\mathbf{v} + \delta\mathbf{v}) - \mathbf{Mv}\|}{\|\mathbf{Mv}\|} \approx \\
&\approx \frac{\|\mathbf{M}\ \delta\mathbf{v} + \delta\mathbf{M}\ \mathbf{v}\|}{\|\mathbf{Mv}\|} \leq \frac{\|\mathbf{M}\|\ \|\mathbf{v}\|}{\|\mathbf{Mv}\|}\ (\epsilon_m + \epsilon_v). \tag{8}
\end{aligned}$$

---

[3] There may actually be an improvement of ϵ_v by adding more transducers with the same individual accuracy, in the sense that more measurements of the same quantities would be available, thus reducing the measurement variance. An equivalent effect could be obtained on the other hand by repeating the measurement of some or all transducers and averaging before solving the equations. We assume for brevity's sake that both those effects are accounted for in evaluating ϵ_v.

In order to give a proper upper limit to the last term of equation 8, which propagates source errors into the computed measurements $\mathbf{Mv}$, it is expedient to consider only vector and matrix 2-norms (i.e. the Euclidean and maximum singular value norm, respectively). It should be pointed out that, although this choice was not specified before for the sake of generality, the use of 2-norms is always advisable in problems like the present one. In fact these norms have the property of being invariant with respect to orthogonal transformations, due e.g. to rigid rotations of the reference frame. On the other hand, being the dimensions of vectors and matrices involved in force sensing small, the computational load is not much larger for 2-norms than for other possible norms. In the following only 2-norms will be considered, and explicit notation will be omitted.

The ratio

$$\frac{\epsilon_{mv}}{\epsilon_m + \epsilon_v} \leq \frac{\|\mathbf{M}\|\|\mathbf{v}\|}{\|\mathbf{Mv}\|} \leq \frac{\|\mathbf{M}\|}{\inf_{\mathbf{v}} \frac{\|\mathbf{Mv}\|}{\|\mathbf{v}\|}} \tag{9}$$

might appear unbound at varying $\mathbf{v}$. In particular, for $\mathbf{v}$ lying in the null space of $\mathbf{M}$, $\mathcal{N}(\mathbf{M})$, infinite amplification of source errors would occur. This corresponds to a choice of $\mathbf{M}$ that neglects every meaningful information from the sensor. More precisely, an upper bound to the ratio 9 can be obtained as follows. Consider the orthogonal decomposition of the vector $\mathbf{v} = \mathbf{v}_p + \mathbf{v}_h$, with $\mathbf{v}_h \in \mathcal{N}(\mathbf{M})$, and $\mathbf{v}_p \in \mathcal{R}(\mathbf{M}^T)$. Using equation 1, we can write $\mathbf{v}_h = \mathbf{C}\,\mathbf{p}_h$. This would not be possible if $\mathbf{v}_h \notin \mathcal{R}(\mathbf{C})$: but in such case $\mathbf{v}_h$ would not correspond to any physically meaningful load configuration, so that it must be $\mathbf{v}_h \in \mathcal{R}(\mathbf{C})$. On the other hand, if we apply equation 5 we have that

$$\mathbf{Mv}_h = 0 = \mathbf{MCp}_h.$$

This equation, along with the previous assumption $\det(\mathbf{MC}) \neq 0$, leads to the conclusion $\mathbf{p}_h = \mathbf{v}_h = 0$.

Since for what has been shown the existence of components of $\mathbf{v}$ belonging to $\mathcal{N}(\mathbf{M})$ can be excluded, equation 9 can be modified to

$$\frac{\epsilon_{mv}}{\epsilon_m + \epsilon_v} \leq \frac{\|\mathbf{M}\|}{\inf_{\mathbf{v}_p} \frac{\|\mathbf{Mv}_p\|}{\|\mathbf{v}_p\|}} = \frac{\|\mathbf{M}\|}{\mu_{min}},$$

where μ_{min} indicates the smallest non-zero singular value of $\mathbf{M}$ (i.e., the square root of the smallest non-zero eigenvalue of $\mathbf{M}^T\mathbf{M}$). It can be easily verified that

$$\frac{\|\mathbf{M}\|}{\mu_{min}} = \|\mathbf{MM}^\dagger\| = N(\mathbf{M}) = N_M,$$

where the obvious generalization of the definition of 2-norm-based condition number to rectangular matrices is introduced [21].

Finally, equation 7 can be restated as

$$\epsilon_p \leq \left\{ \frac{\|\mathbf{M}\|\,\|\mathbf{C}\|}{\|\mathbf{MC}\|}(\epsilon_c + \epsilon_m) + N_M(\epsilon_v + \epsilon_m) \right\} K_p(\mathbf{MC}) = F(\mathbf{C}, \mathbf{M}, \epsilon_v, \epsilon_c, \epsilon_m). \tag{10}$$

This formula is the most general result of this paper. The design objective function $F(\cdot)$ is defined as a function of the compliance matrix $\mathbf{C}$, of the adopted manipulation $\mathbf{M}$, and of the relative source errors ϵ_c, ϵ_v, and ϵ_m. Note that $\mathbf{C}$ and $\mathbf{M}$ are in turn functions of the design variables $\mathbf{x}$. Most often ϵ_m can be expressed in terms of $\mathbf{C}$ and ϵ_c, so that it will be dropped

from the arguments of $F(\cdot)$. Given the values of relative source errors ϵ_v, ϵ_c that are expected with the adopted degree of technological sophistication, the accuracy of force sensors differing in design, solution method and number of transducers (provided that all the transducers have similar statistical properties) can be compared by means of equation 10.

Two particular cases are very important in practice, and are briefly discussed in the following subsections.

5.1 Sensors Solved With Least Squares Methods

A general least-squares approximation of the inconsistent set of equations of a redundant force sensor can be obtained if the choice $\mathbf{M} = \mathbf{W}\mathbf{C}^T$ is made in equation 5, where $\mathbf{W}$ is a diagonal matrix of weights corresponding to different accuracies of basic measurements. Equation 10 can be applied to estimate error propagation in such a sensor. However, since a correct weighting is rarely achievable, the regular least-squares solution with $\mathbf{M} = \mathbf{C}^T$ is the only one currently adopted in practice (see e.g. [15]).

Applying (10) and considering that, for 2-norms, it holds

$$\|\mathbf{C}^T\| = \|\mathbf{C}\|$$

$$\|\mathbf{C}^T\mathbf{C}\| = \|\mathbf{C}\|^2,$$

we have:

$$\epsilon_p \leq \{[2 + N_C]\,\epsilon_c + N_C\epsilon_v\}\,K_p(\mathbf{C}^T\mathbf{C}), \tag{11}$$

where

$$K_p(\mathbf{C}^T\mathbf{C}) = \frac{N_C^2}{1 - 2N_C^2\epsilon_c} \approx N_C^2. \tag{12}$$

Eq.(11) and (12) show how the dependence of sensor accuracy on the condition number is increased for sensors using least-squares approximation [4]. On the other hand, redundant transducers can reduce the condition number N_C. In summary, the effectiveness of redundant transducers should be checked in the specific case, as they may result either beneficial, or useless, or even harmful for sensor precision (this point will be reconsidered later).

5.2 Sensors With Structured Matrices

Some force sensor designs produce compliance matrices whose elements obey to such a pattern that the solution of the associated linear system can be performed very easily. Well contrived sensor designs in fact can realize diagonal or near diagonal $\mathbf{MC}$ matrices, thus decoupling the effect of each load component on the manipulated measurement vector $\mathbf{Mv}$. A good example is described in [5]. Although this concept is not limited to redundant sensors, it is easier to design decoupled sensors when $m > n$.

---

[4]It can be noted that (11) and (12) suggest a more pessimistic estimate of error propagation in least square problems than is currently held in numerical stability analysis [21]. Our bound on error propagation is in effect quite conservative; propagation problems with redundant sensors can be relaxed using more sophisticated algorithms for the inversion of the *normal equation* 5 with $\mathbf{M} = \mathbf{C}^T$, e.g. Householder or SVD methods [23]. More precise bounds would however involve an *a posteriori* evaluation of errors, which is not clearly feasible in our problem. Relations 11 and 12 provide a concise objective function for optimization procedures, whose degree of conservatism is probably of the same order for different designs put in comparison.

Good decoupling was a strict requirement for force sensors designed before the advent of present cheap and powerful electronic computers. In fact, all the data manipulations needed for such sensors could be carried out by simple analog summers and multipliers, most often realized by arranging the Wheatstone bridges and the amplifier gains used for measurement in a peculiar combination. In some cases, for instance when requirements on sensor bandwidth dominate over accuracy needs, such designs can be still today used effectively [20].

The $\mathbf{M}$ manipulation matrix for decoupled sensors consists of a simple pattern of integer numbers, so that we can assume $\delta\mathbf{M} \approx 0$. Eq.(10) can therefore be simplified to the form:

$$\epsilon_p \leq \left\{ \frac{\|\mathbf{M}\| \, \|\mathbf{C}\|}{\|\mathbf{MC}\|}\epsilon_c + N_M \epsilon_v \right\} K_p(\mathbf{MC}). \tag{13}$$

Some interesting conclusions can be drawn from (13). It can be noted for instance that a rescaling of the sensor equations, tending to equilibrate them by multiplying the characteristic matrix by a diagonal weighting matrix $\mathbf{M}$ (which obtains a lower condition number for $\mathbf{MC}$), does not produce any enhancement of sensor accuracy. This fact has obvious physical meaning, and is in effect equivalent to Bauer's theorem, well known in numerical analysis [5] [22].

Furthermore, if sensors are considered as particular redundant sensors, we expect that the objective function calculated with (3) should agree with the one resulting from (10), in its specialized form 13. This can be in fact easily verified by substituting $\mathbf{M} = (\mathbf{I}_{n \times n} | \mathbf{0}_{n \times (m-n)})$ in (13).

Finally, (13) allows us to address the problem raised in section 4, i.e. that the two matrices $\mathbf{C}_1 = \begin{pmatrix} 1 & 0 \\ 0 & 1 \end{pmatrix}$ and $\mathbf{C}_2 = \begin{pmatrix} 1 & 0 \\ 1 & 0 \\ 0 & 1 \end{pmatrix}$ have different condition numbers, although the same information seems, so to say, to be stored in them. The point, which has general validity, is that it makes no sense to consider the objective function value associated with the sensor $\mathbf{C}_2$, without specifying how the equations are going to be solved, i.e. which matrix $\mathbf{M}$ is to be used. So, if we decide to use least squares methods, application of (11) with $\epsilon_c = 0$ gives the objective function value $F(\mathbf{C}_2, \mathbf{C}_2^T, \epsilon_v, \epsilon_c) = 2\sqrt{2}\epsilon_v$, which is much worse than $F(\mathbf{C}_1, \mathbf{I}, \epsilon_v, \epsilon_c) = \epsilon_v$. Yet, a manipulation $\mathbf{M} = \begin{pmatrix} 1 & 0 & 0 \\ 0 & 0 & 1 \end{pmatrix}$ can be applied, such that $F(\mathbf{C}_2, \mathbf{M}, \epsilon_v, \epsilon_c) = \epsilon_v$.

Among the factors that tend to make the decoupling approach obsolete in force sensor design, one is the complexity of mechanical structures necessary to implement it. Design complexity conflicts with requirements on size, cost, and reliability of the sensor. Furthermore, and more subtly, the complexity of structures (where for instance stress concentrations are more or less deliberately introduced), makes the linear model on which the sensor is based less plausible. Besides that, it should be pointed out that force sensors have structured compliance matrices only as far as they are on the designer drawings. No calibration technique is allowed by decoupling design to correct implementation dependent errors on $\mathbf{C}$, so that larger errors ϵ_c must be expected (typically an order of magnitude larger than in calibrated sensors, in the author's experience).

6   Accuracy And Adding More Transducers

Eq.(10) identifies an objective function capable of leading an automatic design procedure in the choice of optimal solutions. Nevertheless, a better understanding of transducer redundancy can

---

[5] Note that this scaling is purely algebraic, as opposed to a weighting based on statistical properties of measurements, which could in fact increase the sensor accuracy, affecting the source error ϵ_v

be gained by analyzing how N_C is varied by adding new transducers.

If $\mathbf{C} \in \Re^{m \times n}$ is the compliance matrix of a given (stage in the design of a) sensor, an additional set of d basic transducers (henceforth called gauges) will produce the new characteristic matrix $\mathbf{A} = \left(\dfrac{\mathbf{C}}{\mathbf{D}} \right)$, where $\mathbf{D} \in \Re^{d \times n}$, $\mathbf{A} \in \Re^{(m+d) \times n}$. The condition number of the new linear system, according to the choice of 2-norms, is the square root of the ratio between the largest and the smallest eigenvalues of $\mathbf{A}^T \mathbf{A}$. Considering $\mathbf{A}^T \mathbf{A}$ as the sum of two symmetric matrices,

$$\mathbf{A}^T \mathbf{A} = \left(\ \mathbf{C}^T \ \big| \ \mathbf{D}^T \ \right) \left(\dfrac{\mathbf{C}}{\mathbf{D}} \right) = \mathbf{C}^T \mathbf{C} + \mathbf{D}^T \mathbf{D},$$

and applying the minimax theorem [23], we have:

$$\frac{\max_{i=1,n}\{\gamma_i^2 + \delta_{n-i+1}^2\}}{\min_{i=1,n}\{\gamma_i^2 + \delta_{n-i+1}^2\}} \leq N_A^2 \leq \frac{\gamma_1^2 + \delta_1^2}{\gamma_n^2 + \delta_n^2}, \tag{14}$$

where $(\gamma_1, \gamma_2, \ldots, \gamma_n)$ and $(\delta_1, \delta_2, \ldots, \delta_n)$ are the singular values of $\mathbf{C}$ and $\mathbf{D}$ in non increasing order, respectively. This relationship gives bounds for condition number variations as a consequence of the addition of new gauges, but it is insufficient to determine whether the variations are favorable or not.

More detailed information can be obtained if extra gauges are added one at a time. The matrix $\mathbf{D}$ in this case is reduced to a row-matrix $\mathbf{d}^T \in \Re^{1 \times n}$, and $\mathbf{D}^T \mathbf{D} = \mathbf{d}^T \mathbf{d} \in \Re^{n \times n}$ has singular values $\delta_1 = (\mathbf{d}^T \mathbf{d})^{1/2}, \delta_2 = \delta_3 = \cdots = \delta_n = 0$. Any set of n orthogonal vectors which includes $\mathbf{d}$ forms an eigenvector set for $\mathbf{D}^T \mathbf{D}$. Eq.(14) is modified in this case as

$$\frac{\max\{\gamma_1^2, \gamma_n^2 + \delta_1^2\}}{\min\{\gamma_{n-1}^2, \gamma_n^2 + \delta_1^2\}} \leq N_A^2 \leq \frac{\gamma_1^2 + \delta_1^2}{\gamma_n^2 + \delta_n^2}.$$

If $\mathbf{d}$ is chosen parallel to the eigenvector of $\mathbf{C}^T \mathbf{C}$ corresponding to the smallest eigenvalue γ_n^2, $\mathbf{C}^T \mathbf{C}$ and $\mathbf{D}^T \mathbf{D}$ share the same eigenvector set. Therefore, also $\mathbf{A}^T \mathbf{A} = \mathbf{C}^T \mathbf{C} + \mathbf{D}^T \mathbf{D}$ shares the same eigenvectors, and the eigenvalues of $\mathbf{A}^T \mathbf{A}$ are equal to those of $\mathbf{C}^T \mathbf{C}$ except for one, $\alpha_s^2 = \gamma_n^2 + \mathbf{d}^T \mathbf{d}$, with $1 < s < n$.

Corresponding to this choice of the direction of $\mathbf{d}$, we have the new condition number:

$$N_A^2 = \frac{\max_{i=1,n} \left\{ \gamma_i^2, \gamma_n^2 + \mathbf{d}^T \mathbf{d} \right\}}{\min_{i=1,n} \left\{ \gamma_{n-i}^2, \gamma_n^2 + \mathbf{d}^T \mathbf{d} \right\}} \geq \frac{\gamma_1^2}{\gamma_{n-1}^2}. \tag{15}$$

According to this result, a new transducer should be placed on the sensor in a position such that its output v_{m+1} is related to the load $\mathbf{p}$ as $v_{m+1} = \mathbf{d}^T \mathbf{p}$, with $\mathbf{d}$ parallel to the singular vector corresponding to the minimum singular value of the old characteristic matrix, and such that $\mathbf{d}^T \mathbf{d} = \gamma_1^2 - \gamma_n^2$. By satisfying perfectly these conditions with $n-1$ additional transducers, it is theoretically possible to modify any given design so as to obtain unitary condition number. In practice, this goal may be impossible to achieve, due to the fact that an arbitrary output law can not always be obtained from a transducer. However, these design suggestions, along with (10), can be useful to decide whether, and how, to correct sensor designs by adding transducers.

7 Applications

In order to illustrate some aspects of the methods above outlined, two applications of optimal force sensor design are presented in this section. The first one is extremely simple, and intended
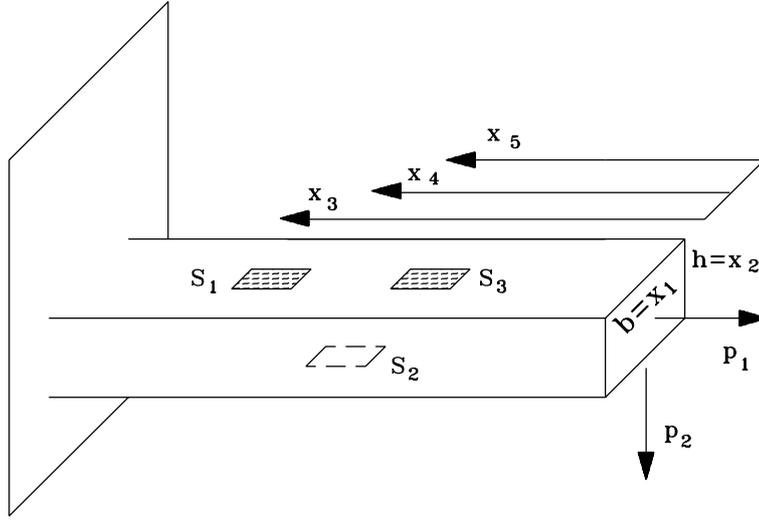
Figure 2: A simple cantilever beam sensor with rectangular cross section.

only for illustrative purposes. The second example reflects a real application problem, regarding the design of miniaturized force sensors designed to fit robotic fingertips. The sensor is currently being produced and successfully employed in several applications.

7.1 A Simple Two Axis Force Sensor

An extremely simple two axis force sensor can be realized as depicted in figure 2. By means of strain measurements on the cantilever beam with rectangular cross section $b \times h$ and length l, the unknown load components p_1 and p_2 are sensed. The five components of the vector $\mathbf{x}$ of design variables are defined as $x_1 = b$, $x_2 = h$, and x_3, x_4, x_5 as the distances of the gauges from the tip of the beam. Three unilateral constraints express limitations on acceptable stress and displacement under the maximum nominal load $\mathbf{p}_{max}$, as well as on the strain under the minimum nominal load $\mathbf{p}_{min}$:

$$
\begin{aligned}
g_1(\mathbf{x}) &= \frac{p_{1,max}}{A} + \frac{p_{2,max}\; l\; x_2}{2J} - \sigma_{adm} \;\leq\; 0, \\
g_2(\mathbf{x}) &= \frac{p_{2,max}l^3}{3EJ} - f_{max} \;\leq\; 0, \\
g_3(\mathbf{x}) &= \frac{p_{1,min}}{EA} - \xi_{min} \;\geq\; 0, \\
g_4(\mathbf{x}) &= \frac{p_{2,min}\; x_2\; x_i}{2EJ} - \xi_{min} \;\geq\; 0, \quad i = 3,5
\end{aligned}
\tag{16}
$$

where $A = x_1 x_2$ is the cross section area, $J = \frac{x_1\; x_2^3}{12}$ its momentum of inertia, E is the Young's modulus of elasticity of the material, and σ_{adm} its maximum admissible strain; f_{max} is the maximum acceptable displacement under load, and ξ_{min} the minimum sensitivity required to the sensor. The feasibility region is defined as

$$
0 \leq x_i \leq l, \quad i = 3,5,
$$

12

while practical bounds are set on $x_1 = b$ and $x_2 = h$ by constructive considerations. Three cases will be considered: a minimal sensor solved with full inversion or with special solution, and a redundant sensor with three basic transducers.

7.1.1 Minimal realization with full inversion

For a minimal sensor using only two gauges, s_1 and s_2, the strains are:

$$\begin{aligned}
v_1 &= \frac{p_{1,max}}{EA}\frac{p_1}{p_{1,max}} + \frac{p_{2,max}x_2}{2EJ}x_3\frac{p_2}{p_{2,max}}, \\
v_2 &= \frac{p_{1,max}}{EA}\frac{p_1}{p_{1,max}} - \frac{p_{2,max}x_2}{2EJ}x_4\frac{p_2}{p_{2,max}}.
\end{aligned}$$

The sensor model is $\mathbf{v} = \mathbf{C}\bar{\mathbf{p}}$, where $\bar{\mathbf{p}} = \left(\frac{p_1}{p_{1,max}} \quad \frac{p_2}{p_{2,max}}\right)$ is the normalized load vector, and the compliance matrix (modulo a constant) is

$$\mathbf{C} = \begin{pmatrix} \frac{p_{1,max}}{EA} & \frac{p_{2,max}x_2x_3}{2EJ} \\ \frac{p_{1,max}}{EA} & -\frac{p_{2,max}x_2x_4}{2EJ} \end{pmatrix}.$$

In this simple case, the optimum design can be easily found. Imposing $N_C = 1$ amounts to an orthogonality condition for the columns of $\mathbf{C}$, $\mathbf{c}_1$ and $\mathbf{c}_2$:

$$\begin{aligned}
\mathbf{c}_1^T\mathbf{c}_2 &= 0, \\
\|\mathbf{c}_1\| &= \|\mathbf{c}_2\|
\end{aligned}$$

whence the design

$$x_3 = x_4 = \frac{x_2}{6}\frac{p_{1,max}}{p_{2,max}}. \tag{17}$$

Given such dimensions the resulting error is $\epsilon_p \approx \epsilon_v + \epsilon_c$. Constrained minimization techniques should be used if these dimensions do not comply with constraints 16.

7.1.2 Minimal realization exploiting the structure of C

If the peculiar structure that $\mathbf{C}$ has for $x_3 = x_4 = x$ is exploited by using a manipulation matrix

$$\mathbf{M} = \begin{pmatrix} 1 & 1 \\ 1 & -1 \end{pmatrix},$$

the original equation is modified to

$$\mathbf{M}\mathbf{v} = \begin{pmatrix} v_1 + v_2 \\ v_1 - v_2 \end{pmatrix} = \mathbf{M}\mathbf{C}\mathbf{p} = \begin{pmatrix} 2\frac{p_{1,max}}{EA} & 0 \\ 0 & \frac{p_{2,max}x_2x}{EJ} \end{pmatrix}\mathbf{p},$$

which can be solved with only $n = 2$ floating-point operations, instead of the $n^2 = 4$ otherwise necessary. This advantage is obviously of some, if little, importance only for larger n than used in this example.

The following relationships can be easily verified:

$$
\begin{aligned}
\|\mathbf{M}\| &= \|\mathbf{M^{-1}}\| = \sqrt{2}; \quad N_M = 1; \\
\|\mathbf{C}\| &= \sqrt{2}\max\left\{ \frac{p_{1,max}}{EA} \ , \ \frac{p_{2,max}x_2 x}{2EJ} \right\}; \\
\|\mathbf{MC}\| &= 2\max\left\{ \frac{p_{1,max}}{EA} \ , \ \frac{p_{2,max}x_2 x}{2EJ} \right\}; \\
N(\mathbf{MC}) &= \max\left\{ \frac{2Jp_{1,max}}{Ap_{2,max}x_2 x} \ , \ \frac{Ap_{2,max}x_2 x}{2Jp_{1,max}} \right\}.
\end{aligned}
$$

According to (13), if $x = \frac{2Jp_{1,max}}{Ap_{2,max}x_2}$ is chosen, we have

$$
\epsilon_p \le \left\{ \frac{\|\mathbf{M}\| \, \|\mathbf{C}\|}{\|\mathbf{MC}\|}\epsilon_c + N_M \epsilon_v \right\} K_p(\mathbf{MC}) \approx \epsilon_v + \epsilon_c,
$$

which shows that this manipulation does not worsen error propagation. However, as already mentioned, in practical cases the cancellation of the off-diagonal entries of $\mathbf{MC}$ is not expected to be perfect, so that larger ϵ_c must be taken into account.

7.1.3 Redundant realization

If the three gauges s_1, s_2, s_3 are placed on the beam, the redundant sensor compliance matrix results

$$
\mathbf{C} = \left(\begin{array}{cc}
\frac{p_{1,max}}{EA} & \frac{p_{2,max}x_2 x_3}{2EJ} \\
\frac{p_{1,max}}{EA} & -\frac{p_{2,max}x_2 x_4}{2EJ} \\
\frac{p_{1,max}}{EA} & \frac{p_{2,max}x_2 x_5}{2EJ}
\end{array} \right).
$$

By imposing $N_C = 1$, we obtain the optimal design:

$$
\begin{aligned}
x_3 - x_4 + x_5 &= 0 && (18) \\
x_3^2 + x_4^2 + x_5^2 &= \frac{3}{144} \frac{p_{1,max}^2 x_2^2}{p_{2,max}^2}, && (19)
\end{aligned}
$$

and, applying (11), we have

$$
\epsilon_p \le 3\epsilon_c + \epsilon_v. \tag{20}
$$

This result shows that the introduction of the third gauge makes error propagation worse. Thus, it is not advisable to add redundant transducers on the sensor in general. However, there may be practical cases where the design given by (17) does not comply with the constraints (16). In such case, the wider design flexibility allowed by the optimality conditions (19) could be advantageously exploited. In order to obtain the final choice, two constrained minimization problems, for the minimal realization and the redundant one respectively, must be solved and the optimal values of ϵ_p compared.

7.2 A Six Axis Miniaturized Force Sensor

As mentioned in the introduction, a particularly promising application of force sensors is intrinsic contact sensing [8]. In its most common embodiment, this method adopts six-axis force sensors integrated as close as possible to the parts of the arm whose surfaces contact the environment. This application has critical size requirements: for instance, force sensors have been designed to fit the interior of fingertips of articulated dextrous hands as small as a cylinder 18mm diameter and 25mm long. Furthermore, contact sensing algorithms use force sensors outputs as input data, thus making accuracy requirements also very important.

The approach to the design of sensors for intrinsic contact sensing that will be illustrated here basically follows the guidelines illustrated below, which we consider in general advisable for high-performance sensor design:

- Use very simple mechanical structures, whose behavior is as close to linear as possible;

- Utilize the least necessary number of transducers, to avoid unnecessary propagation of errors;

- Give the design a convenient parameterization;

- Use numerical techniques to find the best combination of design variables which complies with design constraints.

Following this approach, a miniaturized force sensor has been designed [24] and built in several copies, used to sensorize devices for dextrous manipulation such as the Salisbury hand [25], the "tactile explorator" finger of the Centro "E.Piaggio" [11], and the whole-hand manipulation system UB-Hand II [3]. The mechanical structure of this sensor is sketched in figure 3: it consists of an hollow, thin-walled cylinder. Strain-gauges are applied on the external surface of the cylinder, in a number of six [6]. The cylinder dimensions, the position of the gauges on its structure and their orientation have been considered as the variables to be optimized.

Figure 3 shows the $\{O, \zeta_1, \zeta_2, \zeta_3\}$ reference frame in which the components of the load applied to the sensor extremities are described. The axis ζ_1 is placed along the cylinder axis. The position of the ith gauge is uniquely determined by the cylindrical coordinates of its center point, ζ_{i_1} and θ_i, and by the angle ϕ_i formed by the gauge axis with the cylinder axis. The design variables are three for each gauge, plus the cylinder radius and wall thickness, i.e. 20.

The simplicity of the mechanical structure allows the evaluation of the entries of the compliance matrix $\mathbf{C}$ by means of simple relations of elastic beam theory [26]. Note that the computation of $\mathbf{C}$ has to be done at each iteration step of the numerical optimizing routine, so that avoiding techniques such as the finite element method is extremely expedient. Accordingly, the strain corresponding to the ith gauge is

$$v_i = \sum_{j=1,6} C_{i,j} p_j,$$

where p_j is the value of the jth load component normalized with respect to its nominal maximum value, $p_{j,max}$. Elements $C_{i,j}$ are as follows:

---

[6]This number is actually increased to 7 for temperature compensation; this point is addressed in the appendix.
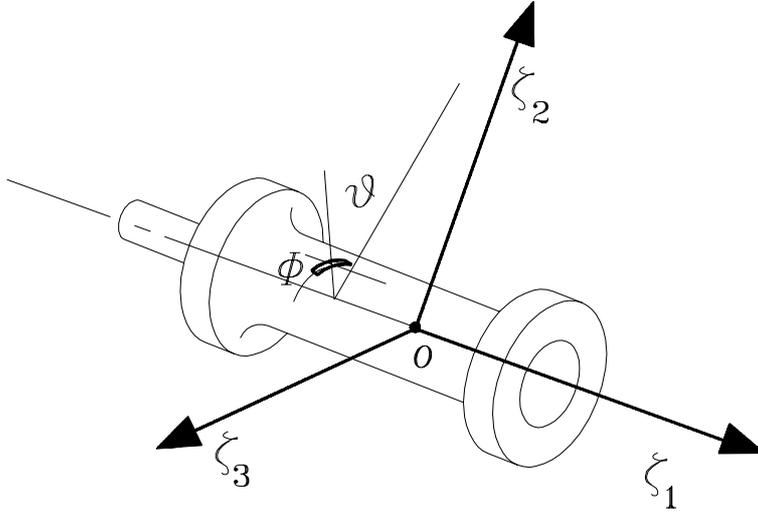
Figure 3: A miniaturized force/torque sensor with cylindrical beam structure.

$$
\begin{aligned}
C_{i,1} &= p_{1,max} W_n (\cos^2 \phi_i - \nu \sin^2 \phi_i); \\
C_{i,2} &= p_{2,max} \left[W_f \zeta_i \cos \theta_i (\cos^2 \phi_i - \nu \sin^2 \phi_i) + W_s \sin \theta_i \sin 2\phi_i \right]; \\
C_{i,3} &= p_{3,max} \left[W_f \zeta_i \sin \theta_i (\cos^2 \phi_i - \nu \sin^2 \phi_i) + W_s \cos \theta_i \sin 2\phi_i \right]; \\
C_{i,4} &= p_{4,max} W_t \sin 2\phi_i; \\
C_{i,5} &= p_{5,max} W_f \cos \theta_i (\cos^2 \phi_i - \nu \sin^2 \phi_i); \\
C_{i,6} &= p_{6,max} W_f \sin \theta_i (\cos^2 \phi_i - \nu \sin^2 \phi_i);
\end{aligned}
$$

where ν is the Poisson's ratio for the structure material, and the moduli W are defined as

$$
\begin{aligned}
W_n &= \frac{1}{2\pi R s E}; \\
W_f &= \frac{2W_n}{R}; \\
W_s &= 2(1+\nu)W_n; \\
W_t &= \frac{(1+\nu)W_n}{R},
\end{aligned}
$$

where E is Young's modulus, R is the cylinder radius and s its wall thickness. The relations above are valid in the assumption $s \ll R$: in this case, $1/s$ is a common factor of $C_{i,j}$, so that N_C is not affected by s. In other words, the relative accuracy of the sensor does not depend on the wall thickness; s can be chosen independently of other design variables, and made such that minimum sensitivity and maximum strain level requirements are met.

Other design constraints for a sensor to fit a robotic hand fingertip are of the form

$$
0 > |\zeta_i - \zeta_j| - l_{max},
$$

$$R_{max} \quad > \quad R > 2s,$$

where $l_{max} = 15mm$, $R_{max} = 6mm$ are typical values.

According to the previous discussion, an objective function $F(R, \zeta_i, \theta_i, \phi_i) = N_C$ has been assumed to optimize this minimal sensor. Note that for minimal sensors, we do not need to use explicit values of the source errors ϵ_v and ϵ_c. The condition number of the compliance matrix is a complex function of the 19 design variables whose minima could not be found analytically. A numerical algorithm (a customized version of Powell's and Broyden's methods [22]) has been employed. The values of design variables corresponding to the lowest of the relative minima found in repeated trials (resulting in $N_{C,min} = 3.07$), are given in table 1. A singular value decomposition of the corresponding compliance matrix is reported in table 2, showing that a 3.07 ratio occurs between the maximum and minimum relative sensitivity, the latter corresponding approximately to the p_1 component of the load, acting along the cylinder axis.

Variable Gage no.	ϕ(rad)	θ(rad)	ζ(mm)	R(mm)	s(mm)
1	0.3	-0.7	1.2		
2	-0.3	1.6	1.7		
3	0.2	3.2	-1.9	5.4	0.2
4	-0.6	-1.8	-1.4		
5	0.4	0.3	-5.9		
6	-0.3	0.9	-6.0		

Table 1: Optimal design variables for the six-axis miniaturized force sensor, corresponding to the nominal load: $p_1 = p_2 = p_3 = 10N$; $p_4 = 60Nmm$; $p_5 = p_6 = 85Nmm$.

	Singular Structure					
Singular values	γ_1 138.4	γ_2 129.6	γ_3 89.4	γ_4 64.3	γ_5 55.9	γ_6 45.0
Singular vectors	$\mathbf{u}_1$	$\mathbf{u}_2$	$\mathbf{u}_3$	$\mathbf{u}_4$	$\mathbf{u}_5$	$\mathbf{u}_6$
	0.07	0.08	0.00	-0.05	-0.27	0.95
	-0.04	0.32	0.83	-0.03	-.17	-0.04
	0.05	-0.36	0.10	0.81	-0.44	-0.05
	0.08	-0.18	0.31	0.34	0.82	0.26
	0.02	0.83	-0.28	0.46	0.10	-0.02
	0.91	0.16	0.34	-0.10	-0.11	-0.12

Table 2: Singular values and corresponding singular vectors of the sensor compliance matrix for the optimal set of design variables listed in table 1.

7.2.1 Sub-optimal design

An interesting sub-optimal configuration of the same force sensor is depicted in figure 4. The centers of the gauges are placed on two circles, on the plane $\zeta_1 = 0$ for gauges 1 through 4, and on the plane $\zeta_1 = -d$ for gauges 5 and 6. Angles are $\theta_i = i\frac{\pi}{2}$, and $\phi_i = (-1)^i \phi$, $1 \leq i \leq 6$.
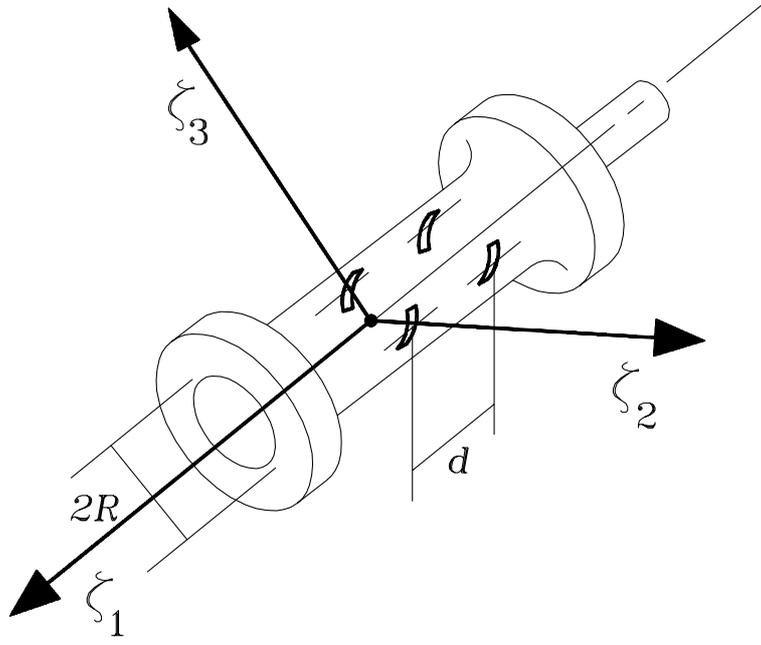
Figure 4: Sub-optimal arrangement of gauges on the miniaturized cylindrical sensor (angles θ and ϕ are defined in figure 3).

Design variables are thus reduced to three, R, d, andϕ. The compliance matrix given by such design has the following structure:

$$\mathbf{C} = \begin{pmatrix} a & 0 & -b & e & 0 & f \\ a & b & 0 & -e & f & 0 \\ a & 0 & b & e & 0 & -f \\ a & -b & 0 & -e & -f & 0 \\ a & c & -b & e & 0 & f \\ a & b & -c & -e & f & 0 \end{pmatrix}.$$

An almost-decoupled sensor can then be obtained even with this extremely simple design, by using a manipulation matrix

$$\mathbf{M} = \begin{pmatrix} 1 & 1 & 1 & 1 & 0 & 0 \\ -1 & 0 & 0 & 0 & 1 & 0 \\ 0 & 1 & 0 & 0 & 0 & -1 \\ 1 & -1 & 1 & -1 & 0 & 0 \\ 0 & 1 & 0 & -1 & 0 & 0 \\ 1 & 0 & -1 & 0 & 0 & 0 \end{pmatrix}.$$

An extremely fast solution of the sensor equations is possible with this arrangement:

$$\mathbf{Mv} = \begin{pmatrix} v_1 & + & v_2 & + & v_3 & + & v_4 \\ v_5 & - & v_1 & & & & \\ v_6 & - & v_2 & & & & \\ v_1 & - & v_2 & + & v_3 & - & v_4 \\ v_2 & - & v_4 & & & & \\ v_1 & - & v_3 & & & & \end{pmatrix} = \begin{pmatrix} 4a & 0 & 0 & 0 & 0 & 0 \\ 0 & c & 0 & 0 & 0 & 0 \\ 0 & 0 & c & 0 & 0 & 0 \\ 0 & 0 & 0 & 4e & 0 & 0 \\ 0 & 2b & 0 & 0 & 2f & 0 \\ 0 & 0 & -2b & 0 & 0 & 2f \end{pmatrix} \mathbf{p}.$$

18

The optimal combination of design variables with sub-optimality constraints is reported in table 3. The corresponding objective function minimum is at $N_C = 6.6$. As expected, the sub-optimal sensor is less accurate than the optimal one. The advantage of this design is that it is possible to choose either a precise solution algorithm (full inversion of C) or a fast one. Perhaps more importantly from a practical point of view, the symmetries of the design render its fabrication much easier than the fully optimized one. It is finally noted that the objective function is fairly smooth in the neighborhood of its minimum, which fact renders the design quite robust to fabrication inaccuracies.

Variable Gage no.	ϕ(rad)	θ(rad)	ζ(mm)	R(mm)	s(mm)
1	0.3	0	-7.9		
2	-0.3	$\pi/2$	-7.9		
3	0.3	π	-7.9	5.6	0.2
4	-0.3	$3\pi/2$	-7.9		
5	0.3	0	4.1		
6	-0.3	$\pi/2$	4.1		

Table 3: Sub-optimal design variables for the six-axis miniaturized force sensor, corresponding to the nominal load: $p_1 = p_2 = p_3 = 10N$; $p_4 = 60Nmm$; $p_5 = p_6 = 85Nmm$.

	Singular Structure					
Singular values	γ_1 121.4	γ_2 121.2	γ_3 65.0	γ_4 60.2	γ_5 32.6	γ_6 32.2
Singular vectors	$\mathbf{u}_1$	$\mathbf{u}_2$	$\mathbf{u}_3$	$\mathbf{u}_4$	$\mathbf{u}_5$	$\mathbf{u}_6$
	0.00	0.07	-0.54	0.00	0.83	0.00
	0.42	0.42	0.49	-0.51	0.28	0.25
	-0.42	0.42	0.49	0.50	0.28	-0.25
	-0.18	0.00	0.00	0.31	0.00	0.93
	0.55	0.56	-0.34	0.44	-0.26	-0.04
	-0.55	0.56	-0.33	-0.43	-0.26	0.04

Table 4: Singular values and corresponding singular vectors of the sensor compliance matrix for the sub-optimal set of design variables listed in table 3.

7.2.2 Some Experimental Data

As already noted, the ultimate performance of a force sensor depends on design quality as well as on technological factors. It is not therefore easy to assess design quality by experimental means, as an extremely large statistical basis, and a tight control of experimental conditions (including details such as quality of gauges, of bonding agents, of electronic components and so on), would be required. Although such exhaustive verification can not be provided here, some numerical values obtained from miniaturized multi-axis sensors will be given for reference.

An aluminum (2024 T4) sensor designed according to the sub-optimal scheme, with wall thickness 0.8mm and using foil-gauge components, has been connected to instrumentation am-
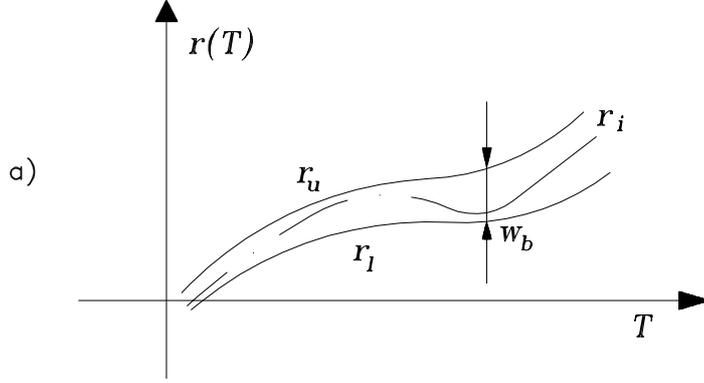
Figure 5: Realization of the miniaturized sensor for the fingertips of a dextrous robot hand. On the left, the force/torque sensor and the fingertip cover. On the right, the fingertips mounted on the fingers of the Salisbury Hand.

plifiers and to an A/D port of a personal computer. The sensor, used for intrinsic contact sensing and designed to fit the fingertips of the Salisbury Hand [25], is shown in figure 5. The maximum nominal load is 30N for force components and 150Nmm for moment components. An estimate of the source error on strain measurements is $\epsilon_v \approx 1\%$, relative to full scale strain. Accurate calibration of the sensor allows to consider $\epsilon_c \approx 1\%$. Acquisition of the unloaded force sensor resulted in floating readings of forces and torques of intensity less than 0.6N and 3.0Nmm, respectively. The minimum detectable load is therefore 2%FSO.

As a figure of the global accuracy of a force/torque sensor, the *cross-talk* matrix $\mathbf{X}$ is sometimes used, whose $X_{i,j}$ entry is defined as the ratio between the measured value of the ith component of the nominal load, p_i, and the actual value p_j (for an ideal sensor, $\mathbf{X} = \mathbf{I}$). The cross-talk matrix obtained for the sensor (employing a full inversion solution scheme) is as follows:

$$
\mathbf{X} = \left(\begin{array}{cccccc}
1.02 & -0.01 & 0.001 & -0.01 & 0.01 & 0.01 \\
0.01 & 1.01 & -0.03 & -0.01 & 0.00 & 0.00 \\
0.01 & 0.01 & 0.99 & 0.05 & 0.00 & 0.01 \\
0.01 & -0.02 & 0.00 & 0.98 & -0.01 & -0.02 \\
0.00 & -0.01 & -0.02 & -0.03 & 1.02 & 0.01 \\
-0.01 & -0.01 & -0.01 & 0.04 & 0.04 & 0.99
\end{array}\right).
$$

Observe that the maximum errors on the diagonal elements of the matrix are in the order of 2%FSO, while spurious readings on non-diagonal terms are larger ($\leq$ 5%FSO). Assuming the maximum norm of the columns of $\mathbf{X}$ as a measure of the relative error, $\epsilon_p = 7.5\%FSO$ can be obtained by this matrix, which is lower than the expected bound $\epsilon_p \leq N_C \ \epsilon_v \epsilon_c \approx 13\%FSO$. This result is believed to depend partly on the conservative nature of the condition number criterion, and partly on the fact that the "worst possible combination" of load components is not reflected in the cross-talk matrix. Being the linearity of basic strain-gages transducers very good in the range of use, the overall sensor linearity is limited by the above figures (5%FSO per

component and 7.5%FSO overall).

8   Conclusions

It has been shown that the design of a multi-axis force sensor can be optimized with respect to its accuracy by minimizing an objective function of the design variables. The proposed function of merit (equation 10) is general enough to allow the choice of the optimal design in a broad range of possible solutions. In particular, the choice of the optimal number of basic transducers to be used in a multi-component sensor is addressed. For sensors employing as many basic transducers as the unknown load components (minimal sensors), the objective function reduces to the condition number of the sensor compliance matrix (equation 3).

An often asked question about multicomponent sensing is: "How many basic transducers should be utilized? Are redundant transducers useful, or useless, or are they harmful to the overal sensor performance?" A clear-cut answer to this question is not possible, since in the general case the direct evaluation of equation 10 is necessary to assess the results. However, a general guideline that results from the discussion of equation 10 is that, whenever the optimal configuration of a minimal sensor complies with the constraints, adding redundant sensors is unlikely to improve sensor accuracy.

Finally, we would like to note that, although multi-axis force sensors have been explicitly considered in this paper, the method proposed is more general, and can be directly extended to any sensor of multiple physical quantities based on a number of linearly related measurements.

Acknowledgments

Appendix: Compensation of Thermal Effects

The various effects of temperature variations are among the most important error sources for basic strain transducers. For resistive strain-gauges, such effects can be grouped, in decreasing order of importance, as follows:

- variation of the intrinsic (non stressed) gauge resistance;

- thermal expansion of the sensor structure;

- gauge-factor variation;

- variation of the elasticity modulus of the structure material.

While the first two phenomena cause errors in measurements v_i, the latter two modify the compliance matrix elements, entering the measurement output in a nonlinear manner. Strain gauges exhibiting a curve of intrinsic resistance vs. temperature that approximately matches (at least in some temperature range) the thermal expansion vs. temperature characteristic curve of the material, are currently available. Such gauges perform a first, rough compensation of thermal effects.

Possible approaches to finer compensation are listed as follows, in increasing order of accuracy:

- To regard the effects of temperature variations ΔT as a component of the source errors. The counteraction is to minimize error propagation;

- To regard nonlinear effects of temperature as source errors, an assume that the remaining effects are functions of the temperature only, independent of the individual gauge characteristics, position, orientation etc. Since the effects of temperature are common to every gauge on the sensor, a dummy gauge applied on a stiff part of the structure, and subject to the same temperature variations, can be taken as a reference.

- To consider nonlinear effects as source errors, and model the remaining effects of temperature T with suitable individual functions $r_i(T)$. These functions are typically approximated by polynomials of degree three or higher. Starting from data normally provided by the gauge supplier, the width $w_b(T)$ of a band within which the r_i of every gauge in the batch employed lies, can be obtained (see figure 6.a). If two curves $r_l(T)$ and $r_u(T)$ are considered such that, for any T and any i, $r_l(T) \leq r_i(T) \leq r_u(T)$, we have:

$$r_u(T) - r_l(T) \leq w_b r_u(T).$$

If moreover an offset measurement is taken at $T = T_0$, the curves $\Delta r_i(T - T_0) = \Delta r_i(\Delta T)$, can be represented as in figure 6.b. Let $\Delta r_m(\Delta T) = \frac{\Delta r_l + \Delta r_u}{2}$ be the median curve of the band, so that any curve Δr_i can be approximated by $\Delta \tilde{r}_i \approx c_{t,i} \Delta r_m(\delta T)$, where $c_{t,i}$ is a constant characteristic of the ith gauge. An upper bound for the approximation error is w_b. The effects of the temperature on a single measurement can be expressed as

$$v_i = \mathbf{c}_i \mathbf{p} + c_{t,i} \Delta r_m(\Delta T),$$

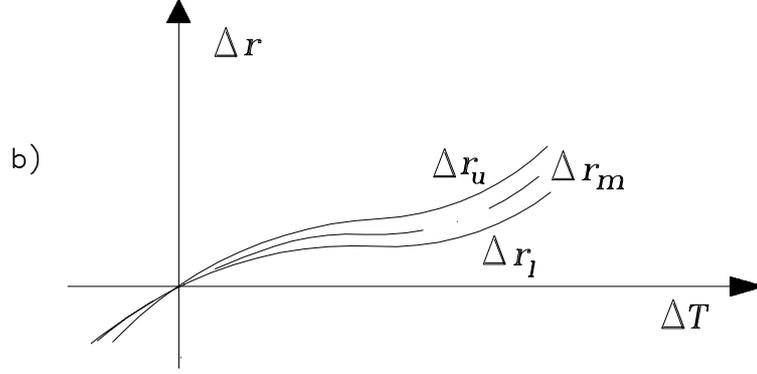where $\mathbf{C}_i$ is the ith row of $\mathbf{C}$. Eq.(10) can therefore be rewritten as

Figure 6: Typical shape of foil gauge resistance vs. temperature curves: a) absolute; b) relative to an offset measurement.

$$\mathbf{v} = \left(\begin{array}{c|c} \mathbf{C} & \mathbf{c}_t \end{array} \right) \left(\dfrac{\mathbf{p}}{\Delta r_m} \right) = \mathbf{C}' \mathbf{p}'.$$

The elements $c_{t,i}$ of the column vector $\mathbf{c}_t$ can be calibrated in controlled temperature conditions. The compensated sensor requires the solution of a linear system of m equations in 7 unknowns. The seventh unknown, Δr_m, is actually of little practical interest, and its calculation can be superseded, as long as the whole calibration matrix has been used to evaluate the non-thermal components of load. The optimization procedures discussed in this paper are still valid for sensor adopting this compensation technique, if applied to the new characteristic matrix $\mathbf{C}'$.

References

[1] E.O. Doebelin: "Measurement Systems Applications and Design," McGraw Hill, chap.5, pp.376-380, 1985.

[2] B.S. Eberman and J. K. Salisbury, "Determination of Manipulator Contact Information from Joint Torque Measurements," Proceedings of the First International Symposium on Experimental Robotics, Montréal, Canada, 1989.

[3] G. Vassura and A. Bicchi: "Whole Hand Manipulation: Design of an Articulated Hand Exploiting All Its Parts to Increase Dexterity," in Robots and Biological Systems, NATO-ASI Series, P.Dario, G.Aebischer, G.Sandini eds., Springer-Verlag, Berlin, RFG, 1989.

[4] P.C. Watson and S.H. Drake: "Pedestal and Wrist Sensors for Automatic Assembly," Proc. 5th Int. Symposium on Industrial Robots, pp.501-511, 1975.

[5] V. Scheinmann: "Preliminary work on Implementing a Manipulator Force Sensing Wrist," AI Lab Report, Stanford University, CA, 1971.

[6] H. VanBrussel, H. Belien, H. Thielemans: "Force Sensing for Advanced Robot Control," Proc. 5th Int. Conf. on Robot Vision and Sensory Control, pp. 59-68, Amsterdam, 1985.

[7] J.K. Salisbury: "Interpretation of Contact Geometries from Force Measurements," Proc. 1st International Symposium on Robotics Research, Bretton Woods, NH. M.Brady and R.Paul Editors, MIT Press, Cambridge, MA, 1984.

[8] A. Bicchi: "Intrinsic Contact Sensing for Soft Fingers," Proc. IEEE Int. Conf. Robotics and Automation, Cincinnati, OH, May 1990.

[9] A. Bicchi, M. Bergamasco, P. Dario, N. Fiorillo: "Integrated Tactile Sensing for Gripper Fingers," Proc. 7th Int. Conf. on Robot Vision and Sensory Control, pp.339-349, Zurich, Switzerland, 1988.

[10] D.L. Brock and S. Chiu: "Environment Perceptions of an Articulated Robot Hand Using Contact Sensors," Proc. ASME Winter Annual Meeting, Miami, FL, 1985.

[11] A. Bicchi and P. Dario: "Intrinsic Tactile Sensing for Artificial Hands," Proc. 4th Int. Symp. on Robotics Research, Santa Barbara, CA. R. Bolles and B. Roth Editors, published by the MIT Press, Cambridge, MA, 1987.

[12] A. Bicchi, J.K. Salisbury, P. Dario: "Augmentation of Grasp Robustness Using Intrinsic Tactile Sensing," Proc. IEEE Conf. on Robotics and Automation, Scottsdale, AZ, 1989.

[13] G.N. Vanderplaats: "Numerical Optimization Techniques," NATO-ASI Series, vol. F27, pp. 197-239, Springer-Verlag, Berlin, RFG, 1987.

[14] M.P. Bendsoe, N.E. Olhoff, J.E. Taylor: "A Variational Formulation for Multi-Criteria Structural Optimization," Journal of Structural Mechanics, vol.11, no.4, 1983.

[15] B.Shimano: "The Kinematic Design and Force Control of Computer Controlled Manipulators," Doctoral Thesis, Stanford University, Stanford, CA, 1978.

[16] E. Isaacson and H.B. Keller: "Analysis of Numerical Methods," J.Wiley and Sons, New York, NY, chap.2, pp. 37-46, 1966.

[17] A.I. Kinchin: "Mathematical Foundations of Information Theory", Dover Publications, NY, 1957.

[18] J.H. Wilkinson: "The Algebraic Eigenvalue Problem," Clarendon Press, Oxford, UK, chap.4 pp.189ff, 1965.

[19] M. Uchiyama and K. Hakomori: "A Few Considerations on Structural Design of Force Sensors," Proc. 3rd Annual Conference on Japanese Robotics Society (in Japanese), 1985.

[20] Y. Nakamura, T. Yoshikawa, I. Futamata: "Design and Signal Processing of Six Axis Force Sensors," Proc. 4th Int. Symp. on Robotics Research, Santa Barbara, CA. R. Bolles and B. Roth Editors, published by the MIT Press, Cambridge, MA, 1987.

[21] G.H. Golub and C.F. VanLoan: " Matrix Computations", Johns Hopkins university Press, Baltimore, MD, 1989.

[22] G. Dahlquist and **r**A. Björk: "Numerical Methods", Prentice Hall, 1974.

[23] G. Strang: "Linear Algebra and its Applications," Harcourt Brace Jovanovich Publ., San Diego, CA, 1988.

[24] "Universal Load Cell with Single Cylindrical Beam," pat. no.67687-a/87 reg. in Turin, Italy, August 1987.

[25] M.T. Mason and J.K. Salisbury: "Robot Hands and the Mechanics of Manipulation," MIT Press, Cambridge, MA, 1985.

[26] S. Timoshenko and D.H. Young: "Theory of Structures," McGraw Hill, NY, 1965.